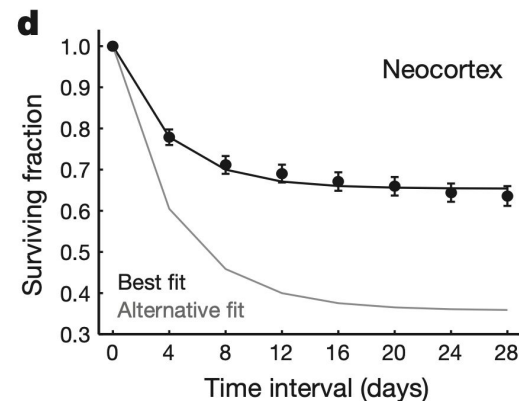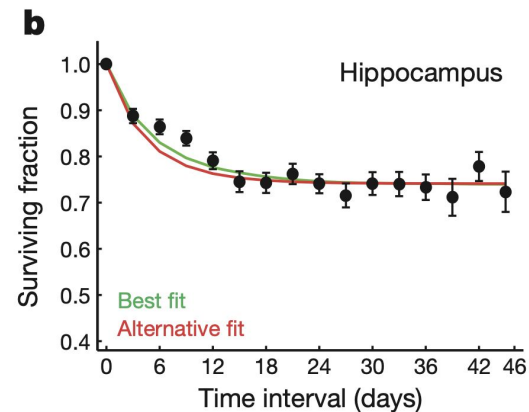# Statistical Physics and Neuronal Weight Decay

—Santanu Rathod

Biological Motivation

In [1] the authors observed the decay of dendritic spines in adult mice and human hippocampus

This is interesting because what it essentially means is that there are some connections that we can get rid of without the loss affecting our day-to-day activities.

Experimental motivation and observation

> It was observed that removing half the weights (or sparsity= 0.5) of a trained single-layered feed-forward neural network doesn't lead to much change in performance (error) as we fit data-points upto a certain point

> However, that wasn't the case for network with half the neurons
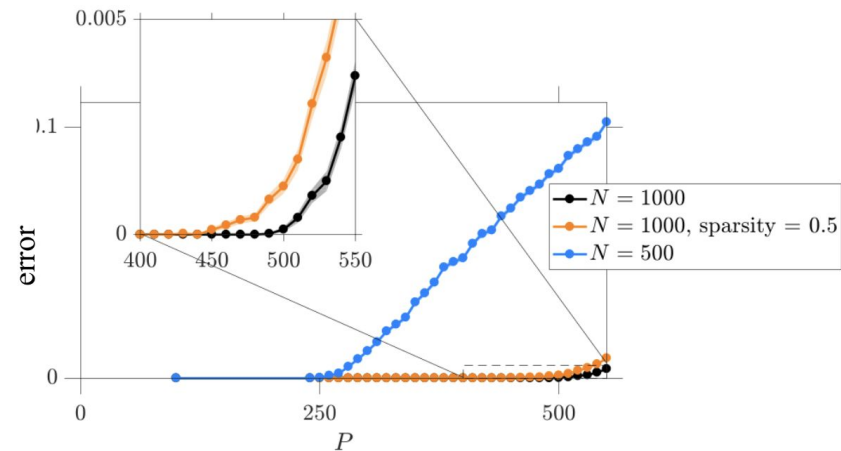
What questions do we need to ask & answer to explain it?

Let **J**= (J_1, J_2, J_3, …, J_N) be one of the solutions, and
let **W**= (J_1, J_2,…, J_(N/2), 0, 0, …, 0) be the sparse (sparsity=0.5) solution

1. What is the relationship between **J** and **W** in the in the context that they have similar performance?

2. Can that relationship be captured via any metric or any term somehow?

3. What role does capacity(P/N) play here? Or what happens as we increase the data-points to fit?
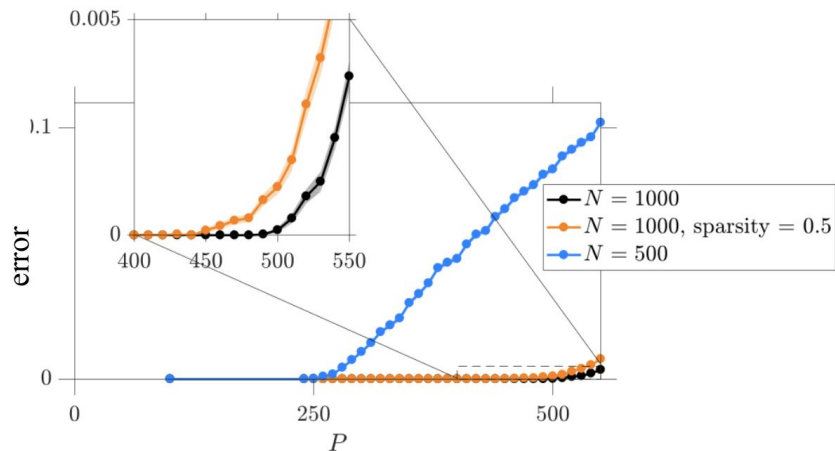
Enter Huang and Kabashima [2]

In their paper titled "**Origin of computational hardness for learning with binary synapses**" [2], Huang and Kabashima explore the relationship between: **Ease of finding solutions vs capacity** in the case of single-layered feed-forward binary perceptrons.

In simpler terms:

1. They showed that as the capacity increases, or as we fit more data-points for a given network, the inter-solution distance increases; with just one solution at max capacity of 0.83

2. For the above result, they explored the relationship between– Franz-Parisi Potential (we'll discuss it later) and solution-distance and capacity
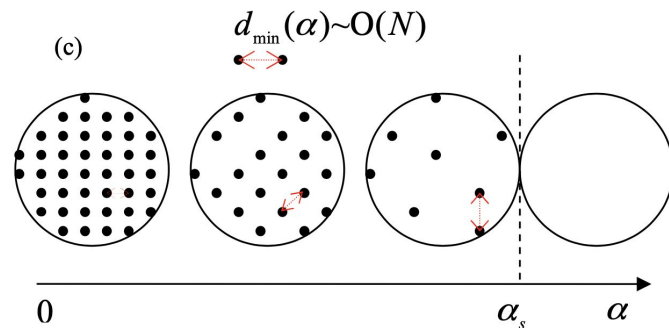
Why can we use Huang and Kabashima's framework to answer our questions?

> **W**= (J_1, J_2,..., J_(N/2), 0, 0, ..., 0), our sparse solution, can be thought of as a co-ordinate transform of **J**= (J_1, J_2, J_3, ..., J_N)

> For our choice of sparsity (e.g. 0.5 above or 0.98) we can get a normalized expected distance E[dist(**J, W**)]/N and use [2]'s framework to explore the relationship between "Sparsity(inter-distance) and Capacity and Franz-Parisi Potential"

> **Although, note that we need to expand the framework to real-space from the discrete binary space.**

Franz-Parisi potential vs Overlap vs Capacity
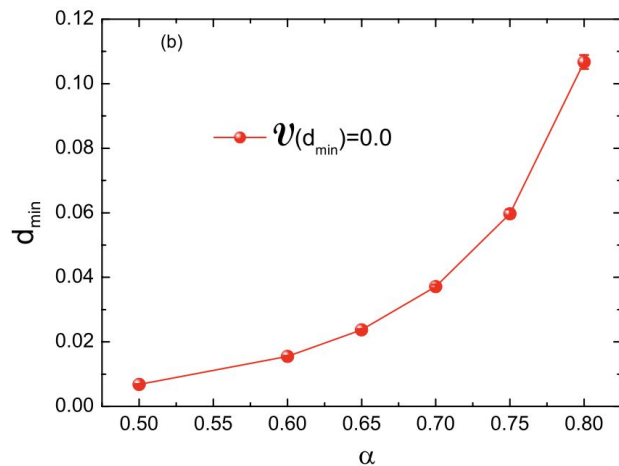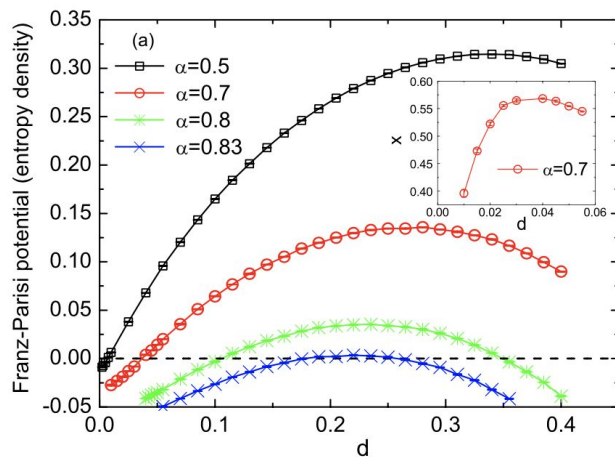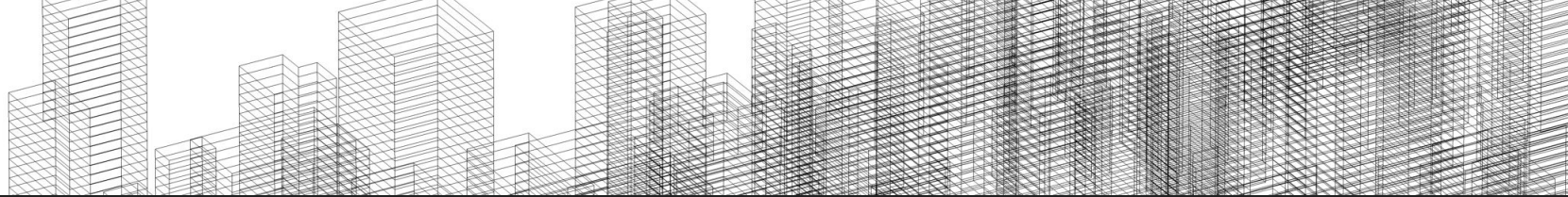
We now define a few terms and elaborate on important steps illustrated in [2] for single-layer BINARY perceptrons

Energy/Classification loss and Free-energy

For a single-layer network with "N" perceptrons, the classification loss or energy over "μ" data-points is defined as:

$$E(\mathbf{J}) = \sum_\mu \Theta \left(-\frac{\sigma_0^\mu}{\sqrt{N}} \sum_{i=1}^N J_i \xi_i^\mu \right)$$

Where J_{i}'s are the weights, σ's are the labels, and $\xi^{\{\mu\}}$'s is the input vector for μ-th data-point

$$F(T, T', x) = \left\langle \frac{1}{Z(T')} \sum_{\mathbf{J}} e^{-\beta' E(\mathbf{J})} \ln \sum_{\mathbf{w}} e^{-\beta E(\mathbf{w}) + x \mathbf{J} \cdot \mathbf{w}} \right\rangle$$

The constrained free-energy above is obtained by first selecting an equilibrium configuration **J** at temperature T', then constrain its overlap with another configuration **w** at a different temperature T. The angular brackets < > above denote average over data-points ξ; the constrained free-energy in the log term is inturn averaged over the configurations **J**

Replica trick

Often in statistical physics formulations we observe terms of the form:

$$Z = \sum_{j=1}^{2^N} \exp\left(-\beta E_j\right)$$

Where the E_{j}'s usually mean the energy for a state configuration and Z usually means the partition function. In our context we're concerned with free-energy density which involves a expected log-partition(E[log(Z)]) term

Replica trick

One can clearly see that logarithm of summations doesn't break down into smaller terms easily; enter the trick:

$$\mathbb{E} \log Z = \lim_{n \to 0} \frac{1}{n} \log(\mathbb{E} Z^n)$$

Where the RHS consists of:

$$Z^n = \sum_{i_1 \ldots i_n = 1}^{2^N} \exp\left(-\beta E_{i_1} - \cdots - \beta E_{i_n}\right)$$

And can be rewritten as:

$$Z^n = \sum_{i_1 \ldots i_n = 1}^{2^N} \prod_{j=1}^{2^N} \exp\left[-\beta E_j \left(\sum_{a=1}^{n} \mathbb{I}(i_a = j)\right)\right]$$

for the ease of calculation

Refined free-energy density

In the lower temperature limit using the tricks: $\ln Z = \lim_{m \to 0} \frac{\partial Z^m}{\partial m}$ and $Z^{-1} = \lim_{n \to 0} Z^{n-1}$ we can modify our free-energy as:

$$F(x) = \lim_{\substack{n \to 0 \\ m \to 0}} \frac{\partial}{\partial m} \left\langle \sum_{\{\mathbf{J}^a, \mathbf{w}^\gamma\}} \prod_\mu \left[\prod_{a,\gamma} \Theta(u_a^\mu) \Theta(v_\gamma^\mu) \right] e^{x \sum_{\gamma, i} J_i^1 w_i^\gamma} \right\rangle$$

where $u_a^\mu \equiv \sum_i J_i^a \xi_i^\mu / \sqrt{N}$ and $v_\gamma^\mu \equiv \sum_i w_i^\gamma \xi_i^\mu / \sqrt{N}$. and we also

need to define the overlap matrixes $Q_{ab} \equiv \mathbf{J}^a \cdot \mathbf{J}^b / N$, $P_{a\gamma} \equiv \mathbf{J}^a \cdot \mathbf{w}^\gamma / N$ and $R_{\gamma\eta} \equiv \mathbf{w}^\gamma \cdot \mathbf{w}^\eta / N$, which characterize the following disorder averages $\langle u_a^\mu u_b^\mu \rangle = Q_{ab}$, $\langle u_a^\mu v_\gamma^\mu \rangle = P_{a\gamma}$ and $\langle v_\gamma^\mu v_\eta^\mu \rangle = R_{\gamma\eta}$. Under the replica symmetric (RS) ansatz, we have $Q_{ab} = q(1 - \delta_{ab}) + \delta_{ab}$, $P_{a\gamma} = p\delta_{a1} + p'(1 - \delta_{a1})$ and $R_{\gamma\eta} = r(1 - \delta_{\gamma\eta}) + \delta_{\gamma\eta}$, where $\delta_{ab} = 1$ if $a = b$ and 0 otherwise.

After (much!!!) algebraic manipulations we get

$$f(x) = \lim_{N \to \infty} F(x)/N = \frac{\hat{r}}{2}(r-1) - p\hat{p} + p'\widehat{p'} + xp + \alpha \int D\omega \int DtH^{-1}(\tilde{t}) \int_{\tilde{t}}^{\infty} Dy \ln H(h(\omega,t,y))$$
$$+ \int D\mathbf{z}(2\cosh\hat{a})^{-1} \left[e^{\hat{a}} \ln 2\cosh(\hat{a}' + \hat{p} - \widehat{p'}) + e^{-\hat{a}} \ln 2\cosh(\hat{a}' - \hat{p} + \widehat{p'}) \right],$$

(4)

where $\int D\mathbf{z} \equiv \int Dz_1 Dz_2 Dz_3$, $\tilde{t} \equiv -\sqrt{\frac{q}{1-q}}t$, and $H(x) \equiv \int_x^{\infty} Dz$ with the Gaussian measure $Dz \equiv G(z)dz$ in which $G(z) \equiv \exp(-z^2/2)/\sqrt{2\pi}$. $h(\omega,t,y) \equiv -\left((p-p')y/\sqrt{1-q} + \sqrt{v_\omega}\omega + p't/\sqrt{q}\right)/\sqrt{1-r}$ where $v_\omega \equiv r - p'^2/q - (p-p')^2/(1-q)$. $\hat{a} \equiv \sqrt{\hat{q} - \widehat{p'}}z_1 + \sqrt{\widehat{p'}}z_3$ and $\hat{a}' \equiv \sqrt{\hat{r} - \widehat{p'}}z_2 + \sqrt{\widehat{p'}}z_3$. The associated self-consistent (saddle-point) equations for the order parameters $\{q, \hat{q}, r, \hat{r}, p, \hat{p}, p', \widehat{p'}\}$ are derived in the Appendix A.

With following associated saddle-point equations:

$$q = \int Dz \tanh^2(\sqrt{\hat{q}}z), \tag{A9a}$$

$$\hat{q} = \frac{\alpha}{1-q} \int Dt \mathcal{R}^2(\tilde{t}), \tag{A9b}$$

$$p = \int D\mathbf{z}(2\cosh\hat{a})^{-1} \left[e^{\hat{a}} \tanh(\hat{a}' + \hat{p} - \widehat{p'}) - e^{-\hat{a}} \tanh(\hat{a}' - \hat{p} + \widehat{p'}) \right], \tag{A9c}$$

$$\hat{p} = x + \frac{\alpha}{\sqrt{(1-q)(1-r)}} \int D\omega \int Dt \mathcal{R}(\tilde{t})\mathcal{R}(h(\omega, t, y = \tilde{t})), \tag{A9d}$$

$$r = \int D\mathbf{z}(2\cosh\hat{a})^{-1} \left[e^{\hat{a}} \tanh^2(\hat{a}' + \hat{p} - \widehat{p'}) + e^{-\hat{a}} \tanh^2(\hat{a}' - \hat{p} + \widehat{p'}) \right], \tag{A9e}$$
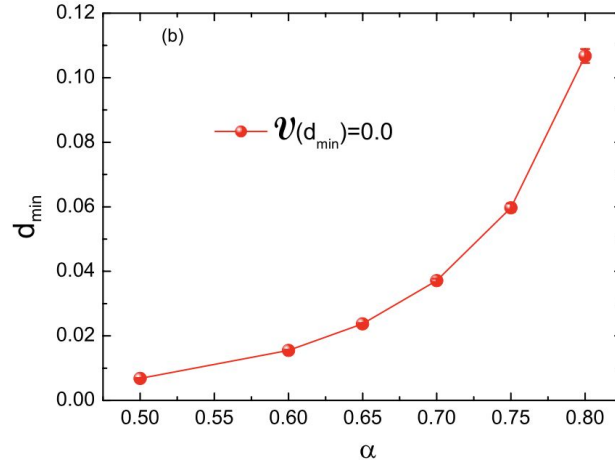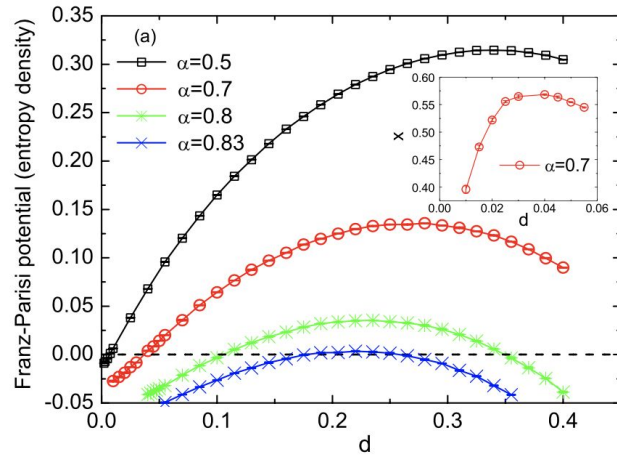
$$\hat{r} = \frac{\alpha}{1-r} \int D\omega \int Dt H^{-1}(\tilde{t}) \int_{\tilde{t}}^{\infty} Dy \mathcal{R}^2(h(\omega, t, y)), \tag{A9f}$$

$$p' = \int D\mathbf{z}(2\cosh\hat{a})^{-1} \left[e^{\hat{a}} \tanh\hat{a} \tanh(\hat{a}' + \hat{p} - \widehat{p'}) + e^{-\hat{a}} \tanh\hat{a} \tanh(\hat{a}' - \hat{p} + \widehat{p'}) \right], \tag{A9g}$$

$$\widehat{p'} = \frac{\alpha}{\sqrt{(1-q)(1-r)}} \int D\omega \int Dt H^{-1}(\tilde{t})\mathcal{R}(\tilde{t}) \int_{\tilde{t}}^{\infty} Dy \mathcal{R}(h(\omega, t, y)), \tag{A9h}$$

Where R(x)= G(x)/H(x) defined in previous slide

Numerically solving those equations gives us:

Constrained free-energy and Franz-Parisi Potential

> The Franz-Parisi potential (FPP) [3] is defined as an effective potential of overlap q between two replicas in two temperatures, T and T′.

>This concept was originally introduced for fully connected spin glass models in order to characterize the one-step replica symmetry breaking (1RSB) as an appearance of the metastable states of a thermodynamic potential.

>A primary advantage of the FPP framework is the ability to describe the 1RSB under the replica symmetric (RS) calculation's level. In addition to its technical ease, this method offers a useful physical insight into what occurs when the replica symmetry is broken. The FPP can also be used to characterize the temperature chaos, to determine the phase diagram of finite-dimensional spin glass [4] etc.

Jolly good, can we get back to neuronal decay?

> So as we just saw Huang and Kabashima's framework helps us comment
on how the solution space looks like in the vicinity of a reference configuration "**J**", and its dependence on capacity and the extent of overlap (distance)

> In neuronal decay we aim to understand
to understand the extent to which pruning
hurts classification performance and its
dependence on P= number of data-points== α*N or dependence on capacity(α)
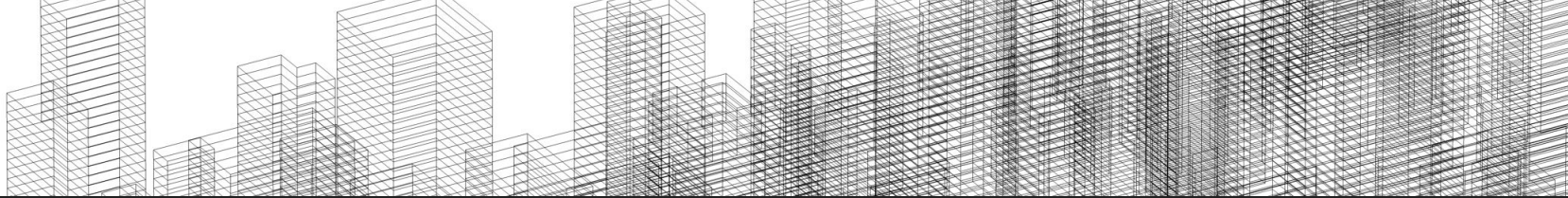
We now extend the
aforementioned framework to
REAL space

Different ways to formulate

Unlike the binary discrete case where for a given dimension the solution space is countably finite, for a real space it's uncountably infinite. There are different ways in which we can tackle it:

1. Assuming that the weights J_{i}~ N(0, 1) such that $\sum_i J_i^2 = N$ or that the solutions lie on a shell of radius sqrt(N)
   a. The assumption is especially valid at capacity
   b. The main advantage of this formulation is that it doesn't introduce extra order parameters as we'll see later
   c. Another advantage is that it gives us a good representation wrt weight decay:

$$
\begin{aligned}
\frac{1}{N} \sum_i J_i w_i &= \int dJ J^2 G(J) \Theta \left(|J| > \Phi^{-1}(\phi) \right) \\
&= 2 \int_{\Phi^{-1}(\phi)}^{\infty} dJ J^2 G(J) \\
&= 2 \left[\Phi^{-1}(\phi) G\left(\Phi^{-1}(\phi) \right) + H\left(\Phi^{-1}(\phi) \right) \right]
\end{aligned}
$$

we thus get a feasible relationship between overlap and pruning

Different ways to formulate

2. When we have no assumption on weights we can get infinite solutions, e.g. if **J** is a solution then so is **cJ** where c>0 is any real constant. We thus normalize our space explicitly or we have: $\sum_i J_i^2 \leq N$
   a. The main advantage here is that the analysis is valid for any both high and low capacity domains.

   b. This formulation however introduces additional complexity both in calculating the free-energy expression as well as adding new order parameters as we'll see ahead

The difference in free-energy expressions

1. Gaussian assumption (solutions on a shell):

$$F(n) = \sqrt{\left[\prod_{a=1}^{n} \int DJ^a \prod_{r=1}^{m} \int Dw^r \cdot \prod_{\mu} \left(\prod_{ar} \theta(v_a^{\mu}) \cdot \theta(v_r^{\mu}) \right) \cdot e^{n J_i^{a_i} \sum_r w^r} \right]}$$

2. Explicit normalization (solutions inside a sphere)

$$F(n) = \sqrt{\left[\prod_{a=1}^{n} \int dJ^a \prod_{j=1}^{m} \int dw^r \cdot \prod_{\mu} \left(\prod_{ar} \theta(v_a^{\mu}) \theta(v_r^{\mu}) \right) \left(\prod_{ar} \theta(F^a) \cdot \theta(F^r) \right) \cdot e^{n J_i^{a_i} \sum_r w^r} \right]}$$

$$\text{where} \quad F^a = 1 - \frac{\sum_{i=1}^{N} (J_i^a)^2}{N} \quad , \quad F^r = 1 - \frac{\sum_{i=1}^{N} (w_i^r)^2}{N}$$

Refined free-energy for Gaussian case

We observe some similarities wrt free energy term for the binary case, for example the triple integral part, but the polynomial term is totally unique in the real case

$$
\begin{aligned}
f\left(x\right) \;=\; & \alpha \int Dt H^{-1}\left(\tilde{t}\right) \int D\omega \int_{\tilde{t}}^{\infty} Dy \log H\left(h\left(\omega, t, y\right)\right) - p\hat{p} + p'\hat{p}' + \frac{r\hat{r}}{2} + xp - \frac{1}{2}\log\left(1 + \hat{r}\right) \\
& + \frac{1}{2\left(1 + \hat{r}\right)}\left[\hat{r} + \frac{\left(\hat{p} - \hat{p}'\right)\left(\hat{p} + \hat{p}' + 2\hat{q}\hat{p}\right)}{\left(1 + \hat{q}\right)^2}\right]
\end{aligned}
$$

(the variables above are similar to the ones defined in binary case from Huang and Kabashima [2])

Final saddle-point equations for Gaussian case

$$\hat{q} = \frac{q}{(1-q)^2}$$

$$\frac{q^2}{1-q} = \alpha \int Dt \mathcal{R}^2 \left(\frac{\sqrt{q}}{\sqrt{1-q}} t \right)$$

$$\hat{p} = x + \frac{\alpha}{\sqrt{(1-q)(1-r)}} \int D\omega \int Dt \mathcal{R} \left(\tilde{t} \right) \mathcal{R} \left(h \left(\omega, t, y = \tilde{t} \right) \right)$$

$$p = \frac{\hat{p} \left(1 + 2\hat{q} \right) - \hat{q} \hat{p}'}{(1+\hat{r})(1+\hat{q})^2}$$

$$\hat{p}' = \frac{\alpha}{\sqrt{(1-q)(1-r)}} \int D\omega \int Dt H^{-1} \left(\tilde{t} \right) \mathcal{R} \left(\tilde{t} \right) \int_{\tilde{t}}^{\infty} Dy \mathcal{R} \left(h \right)$$

$$p' = \frac{\hat{p}' + \hat{q}\hat{p}}{(1+\hat{r})(1+\hat{q})^2}$$

$$\hat{r} = \frac{1}{1-r} \int Dt H^{-1} \left(\tilde{t} \right) \int D\omega \int_{\tilde{t}}^{\infty} Dy \mathcal{R}^2 \left(h \right)$$

$$r = \frac{1}{(1+\hat{r})^2} \left[\hat{r} + \frac{(\hat{p} - \hat{p}')(\hat{p} + \hat{p}' + 2\hat{q}\hat{p})}{(1+\hat{q})^2} \right]$$

Refined free-energy for explicit normalization case

The free-energy term resembles the one from gaussian case albeit with differences in expressions coming from new order parameters

$$f(\eta) = \frac{r\hat{r}}{2} + \hat{p}'\hat{p}' - t\hat{p} + \eta p - \hat{f}(1-\hat{f}) - \frac{1}{2}\log\left(2\hat{f} + \hat{v}\right)$$

$$+ \frac{1}{2} \cdot \frac{1}{\left(2\hat{f}+\hat{v}\right)} * \left[\hat{r} + \frac{\left(\hat{p}-\hat{p}'\right)\left(2\hat{v}\hat{t} + 2\hat{e}\left(\hat{t}+\hat{p}'\right)\right)}{\left(2\hat{e}+\hat{v}\right)^2} \right]$$

$$+ \alpha \int Dt \; H^{-1}(\tilde{f}) \int Dw \int_{\tilde{t}}^{0} Dg \; \log\left(H\left(h(w,t,g)\right)\right)$$

(the variables above are similar to the ones defined in binary case from Huang and Kabashima [2])

Final saddle-point equations for explicit normalization case

- $\hat{a} = \dfrac{q}{(1-q)^2}$

- $\dfrac{q^2}{1-q} = \alpha \int Dt\, R^2\left(\sqrt{\dfrac{q}{1-q}}\; t\right)$

- $\hat{p} = m + \dfrac{\alpha}{\sqrt{(1-q)(1-r)}} \int D\omega \int Dt\, R(\tilde{t})\, R\big(h(\omega, t, y=\tilde{t})\big)$

- $\hat{p}' = \dfrac{\alpha}{\sqrt{(1-q)(1-r)}} \int D\omega \int Dt\, H^{-1}(\tilde{t})\, R(\tilde{t}) \int_{\tilde{t}}^{\infty} Dy\, R(h)$

- $\hat{r} = \dfrac{1}{1-r} \int Dt\, H^{-1}(\tilde{t}) \int D\omega \int_{\tilde{t}}^{\infty} Dy\, R^2(h)$

- $r = \dfrac{1}{(2\hat{f}+\hat{r})^2}\left[\hat{r} + (\hat{p}-\hat{p}')\,\dfrac{(2\hat{a}\hat{p} + 2\hat{e}(\hat{p}+\hat{p}'))}{(2\hat{e}+\hat{a})^2}\right]$

- $\hat{f} = 0$

- $\hat{e} = \dfrac{\hat{a}(\hat{p}'-3\hat{p})}{2(\hat{p}+\hat{p}')}$

- $f = 1 + \dfrac{1}{(2\hat{f}+\hat{r})} + \dfrac{1}{(2\hat{f}+\hat{r})^2}\left[\hat{r} + (\hat{p}-\hat{p}')\,\dfrac{(2\hat{a}\hat{p}+2\hat{e}(\hat{p}+\hat{p}'))}{(2\hat{e}+\hat{a})^2}\right]$

- $p = \dfrac{2\hat{p}(\hat{a}+\hat{e}) - \hat{a}\hat{p}'}{(2\hat{f}+\hat{r})(2\hat{e}+\hat{a})^2}$

- $p' = \dfrac{\hat{a}\hat{p} + 2\hat{e}\hat{p}'}{(2\hat{f}+\hat{r})(2\hat{e}+\hat{a})^2}$

Key Takeaways

1. The intermediary calculations to get the refined free-energy $f(x)$ are huge, hence calculation mistakes are bound to happen
2. One will notice similarities wrt to binary space's case in some expressions, using those expressions as it is will reduce the effort and make your expressions less error prone
3. Usually the authors will skip a lot of intermediary steps, it's helpful to fill in those as similar steps occur frequently
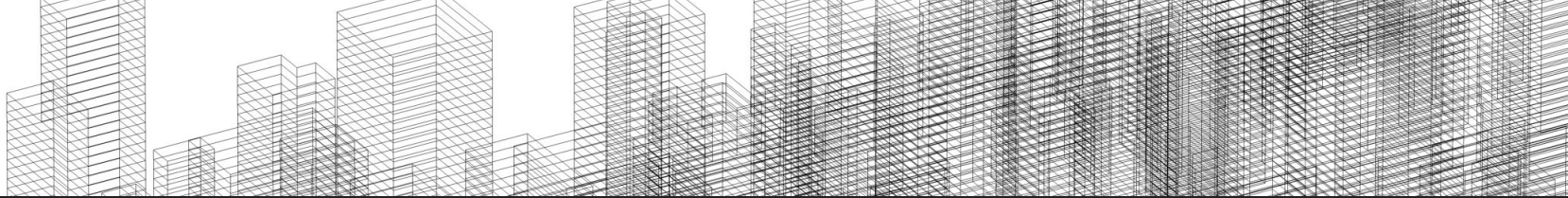
Simulating the saddle-point equations

Main hurdles

1. Double and triple integrals for complicated expressions. Thus a naive numerical integration using Riemannian sum takes a long time
2. Variables leading to undefined expressions
3. Lack of convergence for variables in general
4. Initial runtime was in hours hence debugging too took time

What didn't work

1. Integrating using Riemannian sum
2. Using the integrand expressions as it is (tricks help)
3. Crude updates (always nice to update using a learning parameter η)
4. Writing standard functions on your own, e.g. pdf/cdf/erfc for gaussians etc. (always prefer using standard libraries from matlab/scipy/numpy)

What did work

1. Monte-carlo integration and Rejection sampling
   a. Sample from respective gaussians instead on uniformly sampling or sampling from intervals
   b. Since we have equations like

   $$\hat{r} = \frac{\alpha}{1-r} \int D\omega \int DtH^{-1}(\tilde{t}) \int_{\tilde{t}}^{\infty} Dy \mathcal{R}^2(h(\omega, t, y)),$$

   where "y" depends on "t" use rejection sampling to device a sampler
   distribution to resemble $\Pr(y|t) = \frac{G(y)\Theta(\sqrt{1-q}y+\sqrt{q}t)}{H(-\sqrt{\frac{q}{1-q}}t)}$

2. Clipping undefined regions, e.g. $v_\omega \equiv r - p'^2/q - (p-p')^2/(1-q)$ can take negative values
   hence clipping it to zero helps

Lack of convergence can be frustrating

Debug using:

a. Recheck your equations (common sense)
b. Staring at the expressions, device your own values,
   to see which variable is causing the lack of convergence
c. Check whether your integration method has too much
   variance
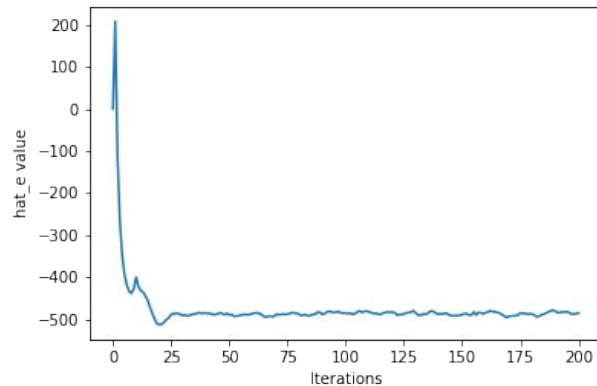d. From (b) above verify is some variable is blowing up other
   variables
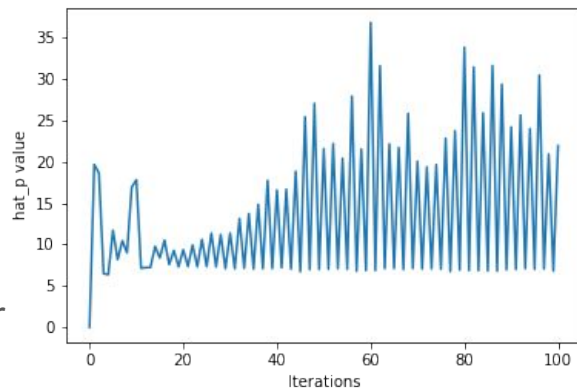
What did work

3. Updating the variables using a learning rate for smooth updates or $x_{t+1} = (1-\eta)x_t + \eta X$ instead of $x_{t+1} = X$, where X: value you get for that iteration:

Before
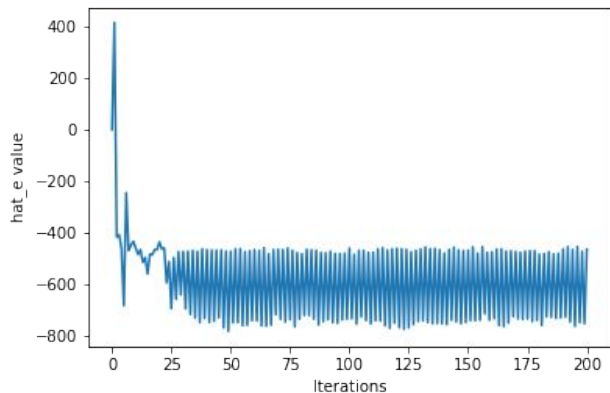
After

Curious case of floating point precision

> Oftentime the terms in your expressions will encounter extreme regions which either take very big or very small values, e.g. 1-cdf(x), x>8, for x~N(0,1)

> Standard floating variables will approximate such values to 1 or 0 or ∞, doing so, at-least in our case, had cascading effects down the line

> It's so because floating numbers are represented using 16/32 bits and sometimes terms might require more bits
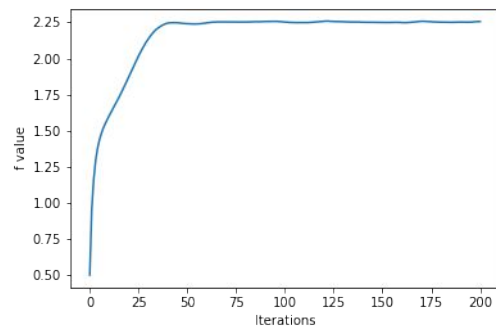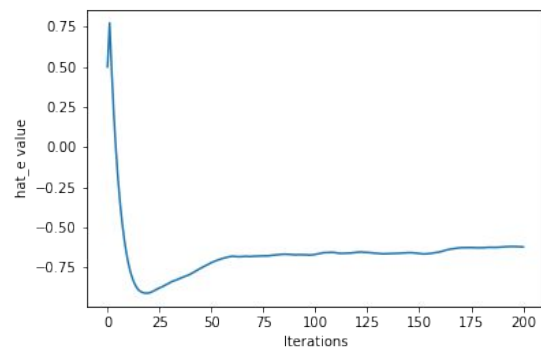
> Thus it's advisable to look whether your terms have already been implemented elsewhere in standard scientific computing libraries scipy/matlab/etc

Convergence

Here are some variable vs iteration graphs. Although only few graphs are shown, we see convergence for all the cases concerned
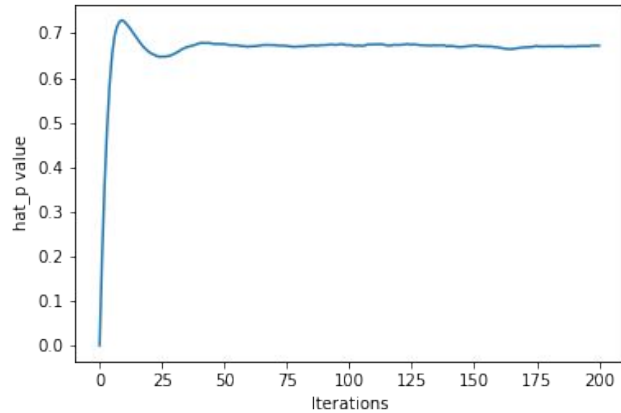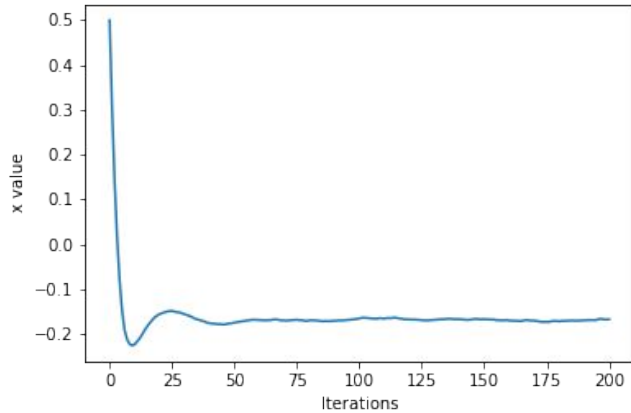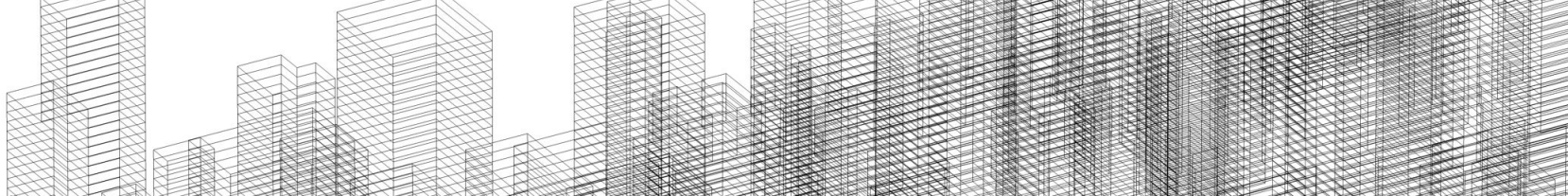
Further steps (soon)

Visualize the Franz-Parisi vs Overlap for real-space case

Thank you!

References

1. Impermanence of dendritic spines in live adult CA1 hippocampus
2. Origin of the computational hardness for learning with binary synapses
3. Franz S and Parisi G, 1995 Journal de Physique I 5 11 1401
4. Caracciolo S, Parisi G, Patarnello S and Sourlas N, 1990 Europhys. Lett. 11 783